



# Transitions between vortex rings, and monopole–antimonopole chains

Jutta Kunz, Ulrike Neemann\*, Yasha Shnir

*Institut für Physik, Universität Oldenburg, Postfach 2503, D-26111 Oldenburg, Germany*

Received 29 June 2006; accepted 17 July 2006

Available online 28 July 2006

Editor: N. Glover

## Abstract

In monopole–antimonopole chain solutions of  $SU(2)$  Yang–Mills–Higgs theory the Higgs field vanishes at  $m$  isolated points along the symmetry axis, whereas in vortex ring solutions the Higgs field vanishes along one or more rings, centered around the symmetry axis. We investigate how these static axially symmetric solutions depend on the strength of the Higgs selfcoupling  $\lambda$ . We show, that as the coupling is getting large, new branches of solutions appear at critical values of  $\lambda$ . Exhibiting a different node structure, these give rise to transitions between vortex rings and monopole–antimonopole chains.

© 2006 Elsevier B.V. Open access under [CC BY license](#).

## 1. Introduction

The nontrivial vacuum structure of  $SU(2)$  Yang–Mills–Higgs (YMH) theory allows for the existence of regular non-perturbative finite mass solutions, such as spherically symmetric monopoles [1], axially symmetric multimono- poles [2–5] and monopole–antimonopole pairs [6,7]. Recently, more general static equilibrium solutions have been constructed, representing either chains of  $m$  alternating monopoles and antimonopoles, carrying charge  $\pm n$ , or vortex ring configurations [8].

The spherically symmetric 't Hooft–Polyakov monopole of unit charge [1] is a topologically stable solution of the field equations. In the Bogomol'nyi–Prasad–Sommerfield (BPS) limit of vanishing Higgs potential axially symmetric multimono- pole configurations are known analytically [4]. In these solutions the nodes of the Higgs field are superimposed at a single point. In the BPS limit repulsive and attractive forces between monopoles exactly compensate and BPS monopoles experience no net interaction [9]. Indeed, calculating the number of zero modes of the configurations shows that they can be con-

tinuously deformed into systems of individual monopoles with unit topological charge [10]. When the Higgs field becomes massive, the fine balance of forces between the monopoles is broken since the corresponding attractive Yukawa interaction becomes short-ranged, and consequently the non-BPS monopoles experience repulsion [5].

As shown by Taubes [11], each topological sector contains besides the (multi)monopole solutions further regular, finite mass solutions, which do not satisfy the first order Bogomol'nyi equations, but only the set of second order field equations, even for vanishing Higgs potential. Such solutions, representing for instance static axially symmetric monopole–antimonopole chain and vortex ring configurations [8], form saddlepoints of the energy functional, and possess a mass above the Bogomol'nyi bound. They exist because the attractive short-range forces between the poles, that are mediated by the  $A_\mu^3$  vector boson and the Higgs boson, are balanced by the repulsion, which is mediated by the massive vector bosons  $A_\mu^\pm$ .

In the topologically trivial sector the simplest of these saddlepoint solutions represents a monopole–antimonopole pair, forming a magnetic dipole [6,7]. When the charge  $\pm n$  of the monopole and antimonopole increases beyond  $n = 2$ , it becomes favourable for the monopole–antimonopole system to form a vortex ring, at least for small values of the Higgs boson mass. Likewise, larger monopole–antimonopole chains then form several vortex rings [8]. For large values of the Higgs

\* Corresponding author.

E-mail address: [neemann@theorie.physik.uni-oldenburg.de](mailto:neemann@theorie.physik.uni-oldenburg.de) (U. Neemann).

boson mass also more complicated configurations can appear, which consist of monopole–antimonopole pairs or chains as well as vortex rings [8]. The presence of an external interaction is also known to change the node structure of a configuration [12].

In the present note we investigate the dependence of such YMH solutions on the strength of the Higgs selfcoupling  $\lambda$ , and thus the value of the Higgs boson mass. We find that, for large values of the Higgs selfcoupling, new branches of equilibrium configurations arise for monopole–antimonopole systems with  $n = 3$ . In particular, we report the existence of new types of solutions with winding number  $n = 3$  and  $m = 2, 3, 4$  and compare their properties to those of the known solutions [8].

In Section 2 we recall  $SU(2)$  YMH theory, and present the axially symmetric Ansatz and the boundary conditions. We then discuss in Section 3 the  $\lambda$ -dependence of the new solutions and their properties.

## 2. $SU(2)$ Yang–Mills–Higgs solutions

### 2.1. Action

We consider  $SU(2)$  Yang–Mills–Higgs theory with action

$$S = \int \left\{ -\frac{1}{2} \text{Tr}(F_{\mu\nu} F^{\mu\nu}) - \frac{1}{4} \text{Tr}(D_\mu \Phi D^\mu \Phi) - \frac{\lambda}{8} \text{Tr}[(\Phi^2 - \eta^2)^2] \right\} d^4x \quad (1)$$

with  $su(2)$  gauge potential  $A_\mu = A_\mu^a \tau^a / 2$ , field strength tensor  $F_{\mu\nu} = \partial_\mu A_\nu - \partial_\nu A_\mu + ie[A_\mu, A_\nu]$ , and covariant derivative of the Higgs field  $D_\mu \Phi = \partial_\mu \Phi + ie[A_\mu, \Phi]$ .  $e$  denotes the gauge coupling constant,  $\eta$  the vacuum expectation value of the Higgs field and  $\lambda$  the strength of the Higgs selfcoupling.

### 2.2. Ansatz

For the gauge and Higgs field we employ the Ansatz [8]

$$A_\mu dx^\mu = \left( \frac{K_1}{r} dr + (1 - K_2) d\theta \right) \frac{\tau_\varphi^{(n)}}{2e} - n \sin \theta \left( K_3 \frac{\tau_r^{(n,m)}}{2e} + (1 - K_4) \frac{\tau_\theta^{(n,m)}}{2e} \right) d\varphi, \quad (2)$$

$$\Phi = \eta (\Phi_1 \tau_r^{(n,m)} + \Phi_2 \tau_\theta^{(n,m)}), \quad (3)$$

where the  $su(2)$  matrices  $\tau_r^{(n,m)}$ ,  $\tau_\theta^{(n,m)}$ , and  $\tau_\varphi^{(n)}$  are defined as products of the spatial unit vectors

$$\begin{aligned} \hat{e}_r^{(n,m)} &= (\sin(m\theta) \cos(n\varphi), \sin(m\theta) \sin(n\varphi), \cos(m\theta)), \\ \hat{e}_\theta^{(n,m)} &= (\cos(m\theta) \cos(n\varphi), \cos(m\theta) \sin(n\varphi), -\sin(m\theta)), \\ \hat{e}_\varphi^{(n)} &= (-\sin(n\varphi), \cos(n\varphi), 0), \end{aligned} \quad (4)$$

with the Pauli matrices  $\tau^a$ .

The four gauge field functions  $K_i$  and two Higgs field functions  $\Phi_i$  depend on the coordinates  $r$  and  $\theta$ , only. With this Ansatz the general field equations reduce to six PDEs in the coordinates  $r$  and  $\theta$ .

The Ansatz possesses a residual  $U(1)$  gauge symmetry. To fix the gauge we impose the condition  $r\partial_r K_1 - \partial_\theta K_2 = 0$  [5]. We further introduce the dimensionless coordinate  $\tilde{x} = er\eta$  and rescale the Higgs field  $\tilde{\Phi} = \Phi/\eta$ .

### 2.3. Boundary conditions

To obtain globally regular solutions with the proper symmetries, we impose appropriate boundary conditions [8].

#### Boundary conditions at the origin

Regularity of the solutions at the origin ( $r = 0$ ) requires the conditions

$$K_1(0, \theta) = K_3(0, \theta) = 0, \quad K_2(0, \theta) = K_4(0, \theta) = 1, \quad (5)$$

$$\sin(m\theta)\Phi_1(0, \theta) + \cos(m\theta)\Phi_2(0, \theta) = 0, \quad (6)$$

$$\partial_r [\cos(m\theta)\Phi_1(r, \theta) - \sin(m\theta)\Phi_2(r, \theta)]|_{r=0} = 0, \quad (7)$$

i.e.  $\Phi_\rho(0, \theta) = 0$ ,  $\partial_r \Phi_z(0, \theta) = 0$ .

#### Boundary conditions at infinity

At infinity we require that solutions in the vacuum sector tend to a gauge transformed trivial solution,

$$\Phi \rightarrow \eta U \tau_z U^\dagger, \quad A_\mu \rightarrow \frac{i}{e} (\partial_\mu U) U^\dagger,$$

and that solutions in the sector with topological charge  $n$  tend to

$$\Phi \rightarrow U \Phi_\infty^{(1,n)} U^\dagger, \quad A_\mu \rightarrow U A_{\mu\infty}^{(1,n)} U^\dagger + \frac{i}{e} (\partial_\mu U) U^\dagger,$$

where

$$\Phi_\infty^{(1,n)} = \eta \tau_r^{(1,n)}, \quad A_{\mu\infty}^{(1,n)} dx^\mu = \frac{\tau_\varphi^{(n)}}{2e} d\theta - n \sin \theta \frac{\tau_\theta^{(1,n)}}{2e} d\varphi$$

is the asymptotic solution of a charge  $n$  multimonopole, and  $U = \exp\{-ik\theta\tau_\varphi^{(n)}\}$ .

In terms of the functions  $K_1 - K_4$ ,  $\Phi_1$ ,  $\Phi_2$  these boundary conditions read

$$K_1 \rightarrow 0, \quad K_2 \rightarrow 1 - m, \quad (8)$$

$$K_3 \rightarrow \frac{\cos \theta - \cos(m\theta)}{\sin \theta}; \quad m \text{ odd},$$

$$K_3 \rightarrow \frac{1 - \cos(m\theta)}{\sin \theta}; \quad m \text{ even}, \quad (9)$$

$$K_4 \rightarrow 1 - \frac{\sin(m\theta)}{\sin \theta}, \quad (10)$$

$$\Phi_1 \rightarrow 1, \quad \Phi_2 \rightarrow 0. \quad (11)$$

#### Boundary conditions along the symmetry axis

The boundary conditions along the  $z$ -axis ( $\theta = 0$  and  $\theta = \pi$ ) are determined by the symmetries,

$$K_1 = K_3 = \Phi_2 = 0, \quad \partial_\theta K_2 = \partial_\theta K_4 = \partial_\theta \Phi_1 = 0. \quad (12)$$

## 3. Numerical results

The numerical calculations are performed with help of the package FIDISOL, based on the Newton–Raphson iterative procedure [13]. We solve the system of 6 coupled non-linear partial differential equation numerically, subject to the above

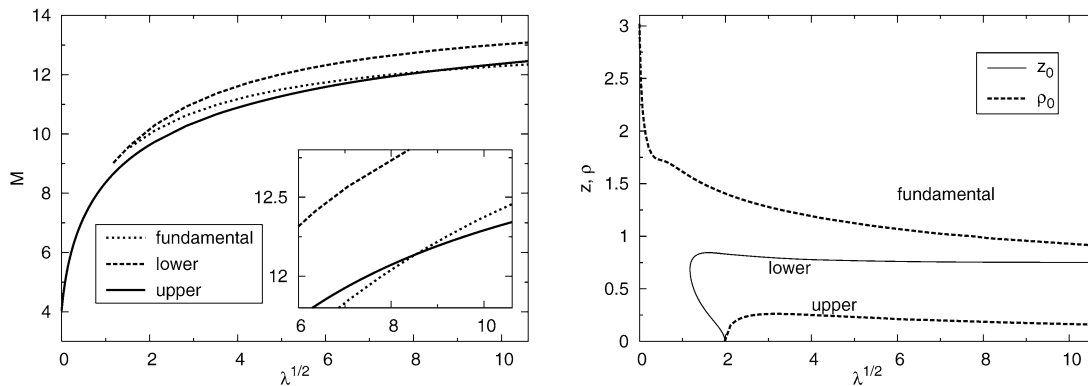


Fig. 1. Left: The mass of the fundamental branch as well as of the new lower (mass) and upper (mass) branch of  $n = 3, m = 2$  solutions versus the Higgs self-coupling  $\lambda$ . Right: The location of the nodes of the Higgs field for the same set of solutions. ( $\rho_0$  denotes the radius of the rings in the  $xy$ -plane,  $z_0$  the location of the isolated nodes on the symmetry axis.)

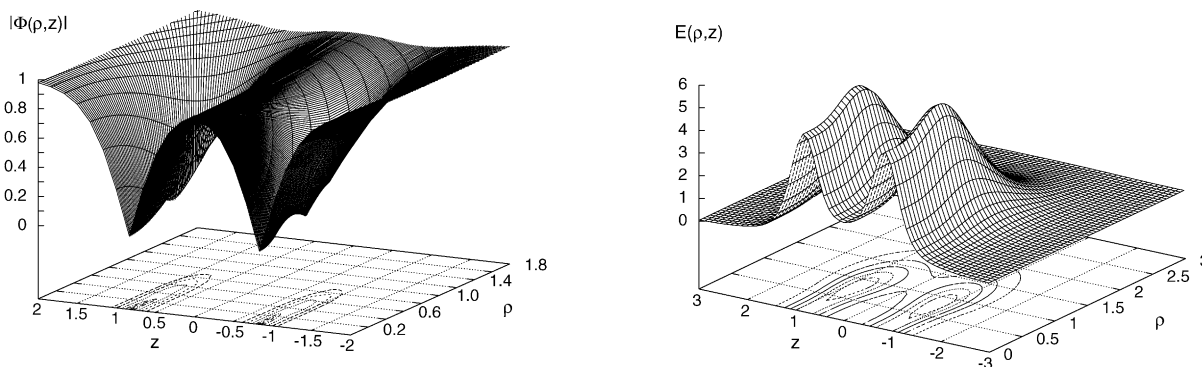


Fig. 2. The modulus of the Higgs field (left) and the energy density (right) of the  $n = 3, m = 2$  solution on the lower branch are shown as functions of the coordinates  $z$  and  $\rho$  for  $\lambda = 2.0$ .

set of boundary conditions, employing the compact radial coordinate  $\bar{x} = \tilde{x}/(1 + \tilde{x}) \in [0 : 1]$ .

We mainly present results for the systems with  $n = 3$  and  $m = 2, 3, 4$ , where all quantities shown are dimensionless. In particular, we illustrate the dependence of the structure of these systems of solutions on the strength of the Higgs self-coupling  $\lambda$ .

In the limit of vanishing and small Higgs self-coupling, these  $n = 3$  solutions have been studied before [8]. When  $m = 2$ , they consist of a single vortex ring in the  $xy$ -plane. When  $m = 3$ , they consist of two opposite vortex rings located symmetrically above and below the  $xy$ -plane together with a triple pole at the origin. When  $m = 4$ , they consist of two like vortex rings located symmetrically above and below the  $xy$ -plane.

As  $\lambda$  is increased from zero, each of these solutions gives rise to a branch of solutions, to which we refer as the respective fundamental branches. Interestingly, at critical values of  $\lambda$ , pairs of new branches of solutions appear, whose node structure differs from the node structure of the solutions of the corresponding fundamental branches.

### 3.1. Topologically trivial sector: $m = 2$ and $m = 4$

$m = 2$ :

Let us start with the simplest case, the  $n = 3, m = 2$  solutions, which possess a single vortex ring along their fundamen-

tal branch. As  $\lambda$  increases, the mass of the solutions increases along the fundamental branch. At the same time, the radius of the single dipole ring in the  $xy$ -plane decreases slowly. The  $\lambda$ -dependence of the mass and the location of the vortex ring  $\rho_0$  of the solutions along the fundamental branch are shown in Fig. 1.

While the fundamental branch persists as  $\lambda$  increases, a new solution appears at a critical value  $\lambda_c^1 = 1.382$ . This solution has higher mass than the fundamental solution, and it has a different node structure: Its Higgs field possesses two isolated nodes on the symmetry axis, representing a monopole–antimonopole pair with charges  $\pm 3$ .

As  $\lambda$  is increased now, two new branches of solutions arise from this critical solution, which differ in mass. The solutions on the lower (mass) branch retain the node structure of the critical solution. Their two isolated nodes on the symmetry axis change only slightly in distance with increasing  $\lambda$ . Their energy density exhibits two tori, whose position is associated with the nodes of the Higgs field, as seen in Fig. 2.

The solutions on the upper (mass) branch, in contrast, do not retain the node structure of the critical solution for long. Their isolated nodes on the symmetry axis approach each other rapidly, and merge at the origin at a second critical value  $\lambda_c^2 = 3.941$ . Thus at  $\lambda_c^2$  we observe a transition from a monopole–antimonopole pair solution to a vortex ring solution. Beyond  $\lambda_c^2$  the radius of the ring first increases rapidly and then

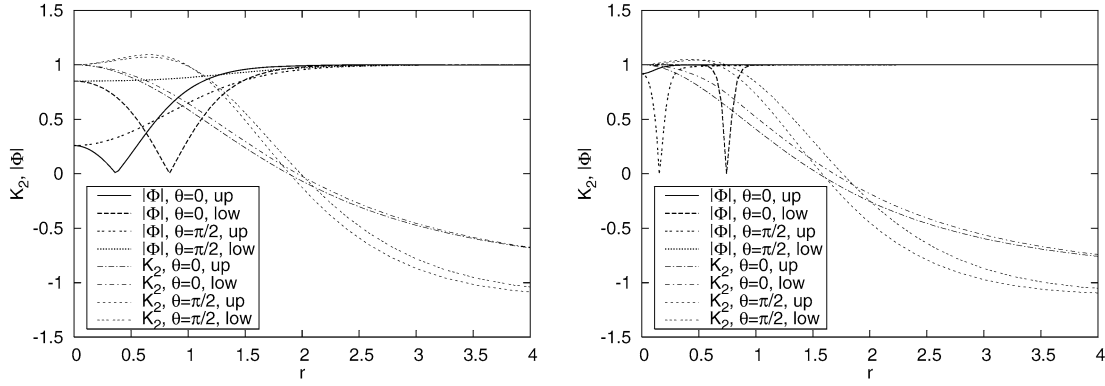


Fig. 3. The modulus of the Higgs field  $\Phi$  and the gauge field function  $K_2$  of  $n = 3$ ,  $m = 2$  solutions on the lower and upper branch are shown as functions of the radial coordinate  $r$  along the  $z$ -axis ( $\theta = 0$ ) and in the  $xy$ -plane ( $\theta = \pi/2$ ) for  $\lambda = 2$  (left) and  $\lambda = 112.5$  (right).

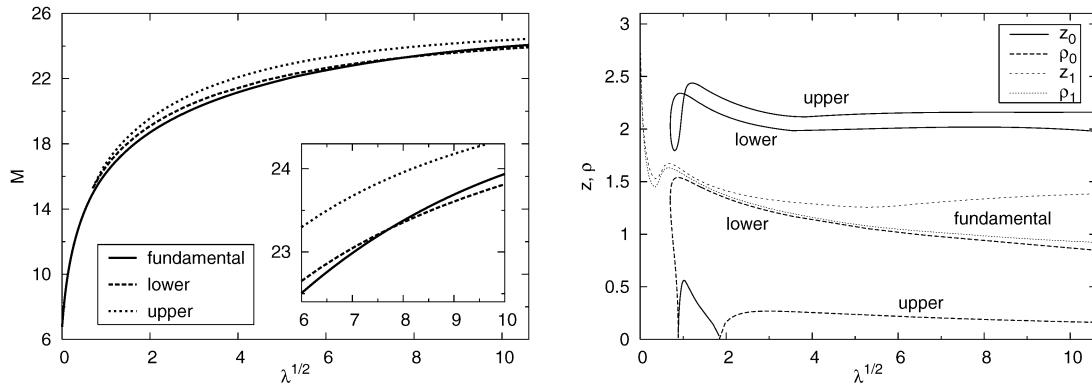


Fig. 4. Left: The mass of the fundamental branch as well as of the new lower (mass) and upper (mass) branch of  $n = 3$ ,  $m = 4$  solutions versus the Higgs selfcoupling  $\lambda$ . Right: The location of the nodes of the Higgs field for the same set of solutions. ( $\rho_0$  denotes the radius of the rings in the  $xy$ -plane,  $z_0$  the location of the isolated nodes on the symmetry axis,  $\rho_1$  and  $z_1$  denote the location of the rings above the  $xy$ -plane.)

decreases slowly again. Both new branches of solutions are also shown in Fig. 1.

We illustrate the new solutions further in Fig. 3, where we exhibit the modulus of the Higgs field  $|\Phi|$  and the gauge function  $K_2$  along the symmetry axis and in the  $xy$ -plane for two values of coupling constant  $\lambda$ . For  $\lambda = 2$  both solutions possess isolated nodes on the symmetry axis, but for the solution on the lower (mass) branch these are farther apart. In contrast, for  $\lambda = 112.5$  the solution on the upper branch has a small ring in the  $xy$ -plane.

Although beyond  $\lambda_c^2$  the new upper branch solutions possess the same node structure as the solutions on the fundamental branch, the size of their vortex ring is much smaller and their mass remains considerably higher. However, since the mass of the new lower branch increases more slowly with  $\lambda$  than the mass of the fundamental branch, a further critical value of  $\lambda$  appears,  $\lambda_c^3 \approx 72.8$ , where the mass of the solution of the fundamental branch coincides with the mass of the solution of the lower branch.  $\lambda_c^3$  thus marks the transition, where it becomes energetically favourable for the field configuration to have two triple nodes on the symmetry axis instead of a single large vortex ring in the  $xy$ -plane.

For larger values of the Higgs selfcoupling the subtle interplay between repulsive and attractive forces thus allows for

more than one non-trivial equilibrium configuration. Analyzing the various contributions to the total mass of these configurations shows, that the kinetic energy of the Higgs field is smallest for the solutions on the fundamental branch (except for a small range of  $\lambda$  close to the first critical point). But the potential energy of the Higgs field and the kinetic energy of the gauge fields are smallest for the solutions on the new lower branch, for larger values of  $\lambda$ . Concerning the total energy balance it then becomes favourable for the Higgs field to form pointlike isolated nodes instead of extended vortex-like nodes, thus causing a transition from a vortex ring to a monopole–antimonopole pair configuration at a critical value of  $\lambda$ .

$m = 4$ :

We now turn to the  $n = 3$ ,  $m = 4$  solutions. The fundamental  $n = 3$ ,  $m = 4$  solutions possess two vortex rings located symmetrically with respect to the  $xy$ -plane. Their radius  $\rho_1$  almost coincides with their distance  $z_1$  from the plane, as seen in Fig. 4. Their location and size varies slowly with  $\lambda$ .

As  $\lambda$  is increased, again a critical value  $\lambda_c^1 = 0.491$  is encountered, where two new branches of solutions arise, possessing higher mass and a different node structure than the solutions on the fundamental branch. The new solutions possess two outer nodes on the symmetry axis, as well as a vortex

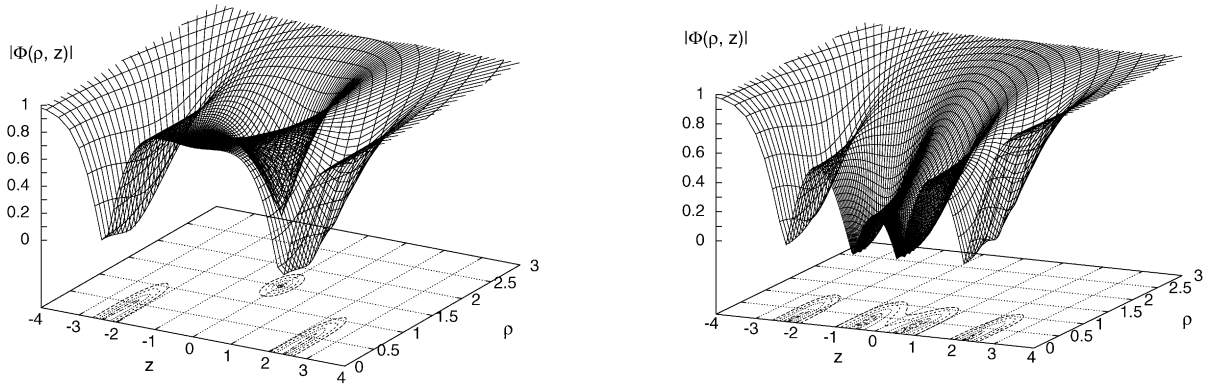


Fig. 5. The modulus of the Higgs field of the lower branch (right) and upper branch (left)  $n = 3, m = 4$  solutions is shown as a function of the coordinates  $z$  and  $\rho$  for  $\lambda = 1$ .

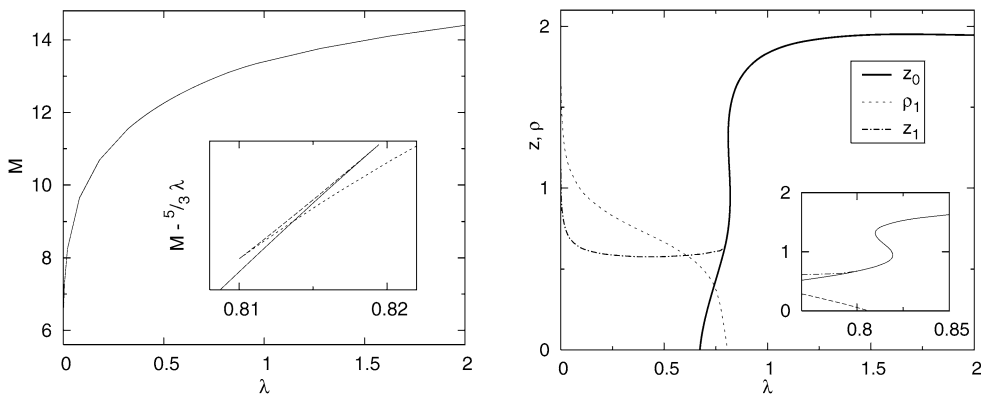


Fig. 6. Left: The mass of the fundamental branch as well as of the new lower (mass) and upper (mass) branch of  $n = 3, m = 3$  solutions versus the Higgs self-coupling  $\lambda$ . Right: The location of the nodes of the Higgs field for the same set of solutions. ( $z_0$  denotes the location of the isolated nodes on the symmetry axis,  $\rho_1$  and  $z_1$  denote the location of the rings above the  $xy$ -plane.)

ring in the  $xy$ -plane. Thus these solutions present a new type of solution with mixed node structure.

With increasing  $\lambda$  the solutions on the lower (mass) branch again retain this node structure, keeping two isolated nodes on the symmetry axis and a vortex ring in the  $xy$ -plane. The solutions on the upper (mass) branch, however, again do not retain this node structure for long. Their single vortex ring in the  $xy$ -plane decreases rapidly in size, and reaches zero size at a second critical value  $\lambda_c^2 = 0.786$ . At  $\lambda_c^2$  we then observe the transition to a monopole–antimonopole chain solution, possessing four isolated nodes on the symmetry axis. Their node structure is illustrated in Fig. 5, where the modulus of the Higgs field is exhibited for both (types of) new solutions at  $\lambda = 1$ .

Interestingly, the new inner nodes approach each other again, and coalesce at the origin at a further critical value,  $\lambda_c^3 = 3.406$ . Beyond  $\lambda_c^3$  the solutions possess again two outer nodes on the symmetry axis, and a small vortex ring in the  $xy$ -plane. The mass and the nodes along the new branches of solutions are also shown in Fig. 4.

Concerning the mass of the new solutions, we again observe a transition between the fundamental branch and the new lower (mass) branch: Beyond  $\lambda_c^4 \approx 59.8$  the new lower branch solu-

tions are energetically favourable, i.e. it becomes again advantageous to exchange vortex rings for isolated nodes. The new lowest mass solution thus contains instead of two vortex rings only a single vortex ring and two nodes on the symmetry axis beyond  $\lambda_c^4$ .

Continuing this reasoning it is tempting to conjecture, that a further critical value of  $\lambda$  might exist, where another pair of branches would appear with now four isolated nodes on the symmetry axis, representing thus monopole–antimonopole chains, and the solutions on this (conjectured) lower (mass) branch would become the energetically most favourable configurations for high values of  $\lambda$ .

### 3.2. Topologically nontrivial sector: $m = 3$

So far we considered solutions of the topologically trivial sector. Let us now address the  $\lambda$ -dependence of solutions in the sector with topological charge  $n = 3$ . For  $\lambda \rightarrow 0$ , the  $n = 3, m = 3$  solutions possess a triply charged monopole at the origin and two oppositely oriented vortex rings located symmetrically above and below the  $xy$ -plane [8].

Based on the observations in the topologically trivial sector we expect a bifurcation at a critical value of  $\lambda$ , where two

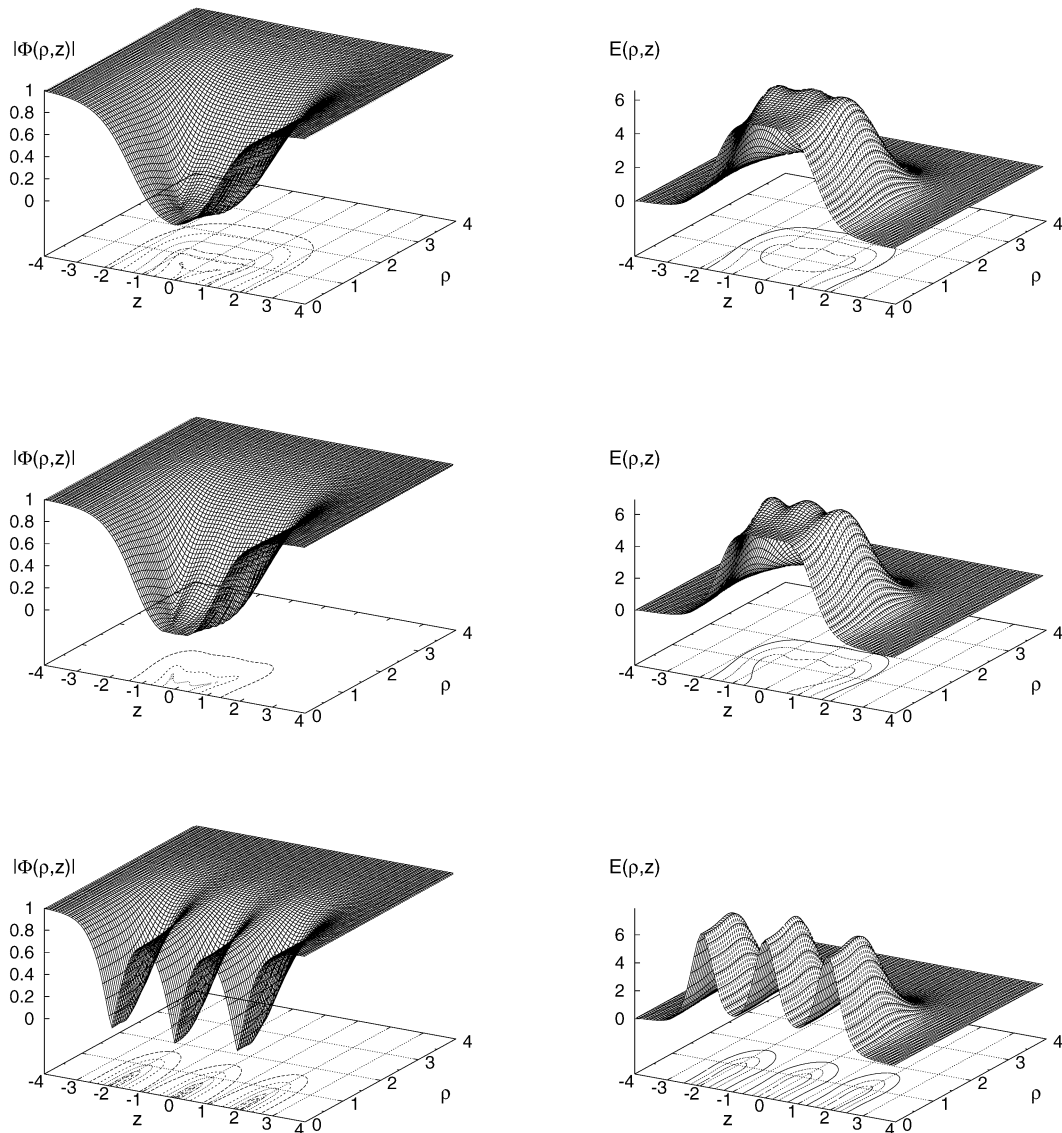


Fig. 7. The modulus of the Higgs field (left) and the energy density (right) of the  $n = 3$ ,  $m = 3$  solutions are shown as functions of the coordinates  $z$  and  $\rho$  for  $\lambda = 0.5$ ,  $\lambda = 0.72$  and  $\lambda = 1.28$ .

new branches of solutions appear, which possess a node structure different from the solutions on the fundamental branch. Furthermore, for high values of  $\lambda$  the energetically most favourable solutions should represent monopole–antimonopole chains.

Constructing the solutions confirms these expectations, but in a surprising way: the node structure of the solutions changes already along the fundamental branch, and the fundamental branch and the new lower branch merge and end at a critical value of  $\lambda$ , while beyond this critical value only the new upper branch persists, as illustrated in Fig. 6.

Considering the  $\lambda$ -dependence of the solutions in detail, we observe that with increasing  $\lambda$  the radius of the vortex rings decreases while the vortex rings first move closer towards each other and then roughly retain their distance. Then, at a critical value  $\lambda_c^1 = 0.673$ , two nodes emerge from

the origin and separate from each other along the  $z$ -axis.<sup>1</sup> Thus beyond  $\lambda_c^1$  the solutions on the fundamental branch possess three nodes on the symmetry axis and two vortex rings located symmetrically above and below the  $xy$ -plane. As  $\lambda$  increases further, the new nodes move further apart, while the vortex rings shrink to zero size and merge with the new nodes on the  $z$ -axis at a critical value  $\lambda_c^2 = 0.807$ . Beyond  $\lambda_c^2$ , the solutions possess only three isolated nodes on the symmetry axis and represent monopole–antimonopole chains.<sup>2</sup>

<sup>1</sup> These new nodes appear to be encircled by tiny rings not exhibited in Fig. 6.

<sup>2</sup> The  $\lambda$ -dependence of the nodes of the solutions with fixed  $n = 3$  and  $m = 3$  is very similar to the  $n$ -dependence of the nodes of the solutions with fixed  $\lambda = 0$  and  $m = 3$  [8].

We note though, that for a small range of  $\lambda$ ,  $0.810 \leq \lambda \leq 0.819$ , three branches of solutions are present, as seen in Fig. 6. Clearly, at  $\lambda_c^3 = 0.810$  two new branches of solutions appear which possess the node structure of monopole–antimonopole chains. The new lower branch then merges with the fundamental branch at  $\lambda_c^4 = 0.819$ , where both branches end, while the upper branch extends to high values of  $\lambda$ . The modulus of the Higgs field and the energy density of several  $n = 3$ ,  $m = 3$  solutions are illustrated in Fig. 7.

#### 4. Conclusions

We have investigated static axially symmetric solutions of the  $SU(2)$  Yang–Mills–Higgs theory, representing monopole–antimonopole chains and vortex rings, and obtained new types of solutions, representing mixed chain–vortex ring configurations.

Starting from vortex ring solutions in the limit of vanishing Higgs selfcoupling constant  $\lambda$ , we observe that at critical values of  $\lambda$  pairs of new branches of solutions appear. Thus for larger values of  $\lambda$  the subtle interplay between repulsive and attractive forces allows for more than one non-trivial equilibrium configuration of these systems.

The new branches of solutions possess a different node structure, where, in particular, vortex rings are replaced by isolated nodes on the symmetry axis. For high values of  $\lambda$  these new solutions have the lowest mass.

While we have studied here in detail only the systems with  $n = 3$  and  $m = 2, 3, 4$ , we conjecture, that this phenomenon is not restricted to these particular systems but that it is of a more general nature, implicating an enormous richness of configuration space for high values of  $\lambda$ .

Finally, it appears interesting to consider the effects of gravity on these new types of solutions, and thus to obtain the gravitating analog of these regular solutions as well as the corresponding non-Abelian black holes solutions, if they exist [14–17].

#### Acknowledgements

We would like to acknowledge valuable discussions with Burkhard Kleihaus, Stephane Nonnemacher, Eugen Radu and Tigran Tchrakian.

#### References

- [1] G. 't Hooft, Nucl. Phys. B 79 (1974) 276; A.M. Polyakov, Pis'ma JETP 20 (1974) 430.
- [2] E.J. Weinberg, A.H. Guth, Phys. Rev. D 14 (1976) 1660.
- [3] C. Rebbi, P. Rossi, Phys. Rev. D 22 (1980) 2010.
- [4] R.S. Ward, Commun. Math. Phys. 79 (1981) 317; P. Forgacs, Z. Horvath, L. Palla, Phys. Lett. B 99 (1981) 232; M.K. Prasad, Commun. Math. Phys. 80 (1981) 137; M.K. Prasad, P. Rossi, Phys. Rev. D 24 (1981) 2182.
- [5] B. Kleihaus, J. Kunz, D.H. Tchrakian, Mod. Phys. Lett. A 13 (1998) 2523.
- [6] B. Rüber, Thesis, University of Bonn, 1985.
- [7] B. Kleihaus, J. Kunz, Phys. Rev. D 61 (2000) 025003.
- [8] B. Kleihaus, J. Kunz, Ya. Shnir, Phys. Lett. B 570 (2003) 237; B. Kleihaus, J. Kunz, Ya. Shnir, Phys. Rev. D 68 (2003) 101701; B. Kleihaus, J. Kunz, Ya. Shnir, Phys. Rev. D 70 (2004) 065010.
- [9] N.S. Manton, Nucl. Phys. B 126 (1977) 525; W. Nahm, Phys. Lett. B 85 (1979) 373; N.S. Manton, Phys. Lett. B 154 (1985) 397.
- [10] E.J. Weinberg, Phys. Rev. D 20 (1979) 936.
- [11] C.H. Taubes, Commun. Math. Phys. 86 (1982) 257; C.H. Taubes, Commun. Math. Phys. 86 (1982) 299; C.H. Taubes, Commun. Math. Phys. 97 (1985) 473.
- [12] Ya Shnir, Phys. Rev. D 72 (2005) 055016.
- [13] W. Schönauer, R. Weiß, J. Comput. Appl. Math. 27 (1989) 279; M. Schauder, R. Weiß, W. Schönauer, The CADSOL Program Package, Universität Karlsruhe, Interner Bericht Nr. 46/92, 1992.
- [14] K. Lee, V.P. Nair, E.J. Weinberg, Phys. Rev. D 45 (1992) 2751; P. Breitenlohner, P. Forgacs, D. Maison, Nucl. Phys. B 383 (1992) 357; P. Breitenlohner, P. Forgacs, D. Maison, Nucl. Phys. B 442 (1995) 126.
- [15] B. Hartmann, B. Kleihaus, J. Kunz, Phys. Rev. Lett. 86 (2001) 1422; B. Hartmann, B. Kleihaus, J. Kunz, Phys. Rev. D 65 (2001) 024027.
- [16] B. Kleihaus, J. Kunz, Phys. Rev. Lett. 85 (2000) 2430; B. Kleihaus, J. Kunz, Ya. Shnir, Phys. Rev. D 71 (2005) 024013.
- [17] R. Ibádov, B. Kleihaus, J. Kunz, Y. Shnir, Phys. Lett. B 609 (2005) 150; B. Kleihaus, J. Kunz, U. Neemann, Phys. Lett. B 623 (2005) 171.